



Efficient iris segmentation method in unconstrained environments



Shaaban A. Sahmoud*, Ibrahim S. Abuhaiba

Islamic University of Gaza, Jameaa street, Islamic University, Gaza 972, Palestine

ARTICLE INFO

Article history:

Received 16 July 2012

Received in revised form

31 March 2013

Accepted 2 June 2013

Available online 15 June 2013

Keywords:

Biometrics

Iris recognition

Iris segmentation

Non-cooperative iris recognition

Eyelid localization

ABSTRACT

Recently, iris recognition systems have gained increased attention especially in non-cooperative environments. One of the crucial steps in the iris recognition system is the iris segmentation because it significantly affects the accuracy of the feature extraction and iris matching steps. Traditional iris segmentation methods provide excellent results when iris images are captured using near infrared cameras under ideal imaging conditions, but the accuracy of these algorithms significantly decreases when the iris images are taken in visible wavelength under non-ideal imaging conditions. In this paper, a new algorithm is proposed to segments iris images captured in visible wavelength under unconstrained environments. The proposed algorithm reduces the error percentage even in the presence of types of noise include iris obstructions and specular reflection. The proposed algorithm starts with determining the expected region of the iris using the K-means clustering algorithm. The Circular Hough Transform (CHT) is then employed in order to estimate the iris radius and center. A new efficient algorithm is developed to detect and isolate the upper eyelids. Finally, the non-iris regions are removed. Results of applying the proposed algorithm on UBIRIS iris image databases demonstrate that it improves the segmentation accuracy and time.

© 2013 Elsevier Ltd. All rights reserved.

1. Introduction

With an increasing attention to security, the need for an automatic personal identification system based on biometrics has increased because traditional identification systems based on cards or passwords can be broken by losing cards, stealing them or forgetting passwords. Iris recognition is becoming one of the most important biometrics used in recognition. This importance is due to its high reliability for personal identification [1–3]. Human iris patterns are very stable throughout a person's life [4,5]. Furthermore, each iris is unique and even irises of identical twins are also different. This is because the human iris is a complex pattern and contains many distinctive features such as arching ligaments, furrows, ridges, crypts, rings, freckles and a zigzag collarette, thus iris patterns possess a high degree of randomness.

Since the concept of automatic iris recognition was proposed in 1987 [4], many researchers have proposed a lot of powerful algorithms in this field. Most of these algorithms need user cooperation to get a high-quality image and to provide the users with feedback to ensure that they are properly positioned for image capture. The most relevant algorithms and widely used in current real applications are those developed by Daugman, which require NIF camera to capture the iris images.

When current iris recognition algorithms deal with noisy iris images taken in visible wavelength under non-ideal imaging conditions, the algorithms accuracy significantly decreases because the segmentation stage is much affected with noise and non-ideal lighting conditions. Fig. 1(a) shows an image taken under ideal conditions with NIF camera, where the image in Fig. 1(b) was taken in visible wavelength under non-ideal conditions, and thus it is extremely challenging to segmentation process.

The main motivation in this paper is to propose a robust iris segmentation algorithm able to deal with highly noisy iris images captured under unconstrained conditions and non-ideal environments, which cannot be handled using current iris segmentation algorithms such as Daugman algorithms. The CHT is the best circles localizing operator in the noisy images but it is very expensive in time. Therefore, the proposed algorithm adds a new pre-processing step using K-means algorithm to divide the iris image into three regions namely iris region, skin region and sclera region. The K-means pre-processing step could exclude the non-iris regions which cause many errors and decrease the searching time of the CHT. Furthermore, a number of new methods are proposed to enhance the performance of the segmentation in noisy images such as a method to localize the upper eyelid through detecting it in the sclera region as that will enable the algorithm to deal more effectively with noisy iris images. The proposed algorithm segments the noisy iris images and reduces the execution time, enabling it to be used in real-time applications.

The rest of the paper is organized as follow. Section 2 describes a brief survey of related work in iris segmentation. Section 3

* Corresponding author. Tel.: +972 59 5800875.

E-mail addresses: shaaban.sahm@gmail.com, ssahmoud1@students.iugaza.edu (S.A. Sahmoud).

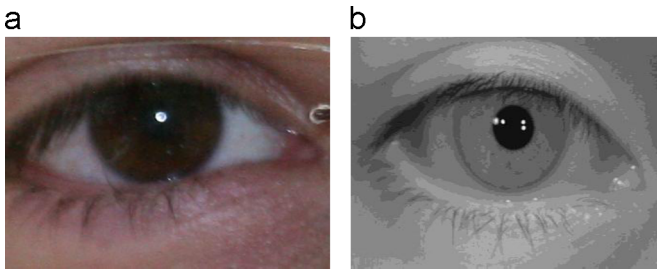


Fig. 1. Comparison of iris images from the UBIRIS.v2 and CASIA (version 4). (a) image from the UBIRIS.v2. (b) image from CASIA (version 4).

explain the proposed iris segmentation algorithm. Experimental results are represented in [Section 4](#) and [Section 5](#) concludes the paper. References have been mentioned in [Section 6](#).

2. Related work

Many researchers have much contributed in iris segmentation [6]. They have used different techniques to increase the performance of their algorithms. Previous algorithms have been classified according to two criteria. The first classification is according to the region of starting in segmentation, whereas the second is according to the operators or techniques used in describing the shapes inside the eye. In this section, we present the most prominent works in these two classification.

2.1. The region of starting the segmentation

There are three categories of researchers depending on where do they start the segmentation. The first category of researchers starts from pupil [7,8] because it is the darkest region in the image. Based on this fact, pupil is localized first, and then the iris is determined using different techniques. Finally, noises are detected and isolated from the iris region. In the second category [9], the segmentation starts from the sclera region because it is found to be less saturated (white) than other parts of the eye and then the iris is detected using any type of operators. Finally, the pupil and noises are detected and isolated from iris region. The third category [10,11] of researchers searches for the iris region directly by using edge operators or applying clustering algorithms to extract iris texture features.

2.2. The techniques used to describe the shapes inside the eye

According to the techniques and operators that are used in iris segmentation, there are two common approaches used in localizing the iris region. The first approach [12,13] applies a type of edge detection followed by CHT or one of its derivatives to detect the shape of iris and pupil. A final stage can be applied to correct the shape of iris or pupil. The main problem with this approach is that the CHT is practically very expensive in time. The second approach [7,14–16] uses different types of operators to detect the edges of iris like Daugman Integro-Differential operator [17] or Camus and Wildes [18] operator and then the pupil and noises are detected and isolated. However, these operators are affected by noises and separability between iris and sclera. As a result, it could not be used with noisy iris images.

3. Overview of the proposed approach

The proposed segmentation algorithm avoids starting from the pupil because it is not always the darkest region in the noisy iris

images taken in a visible wavelength. Further, the algorithm avoids starting from sclera because it can be covered by dark colors which cause errors in determining the iris region and thus in segmentation process.

The algorithm starts by determining the expected region of iris using K-means clustering algorithm and then, vertical Canny edge detection is applied on the output image to produce edge-maps. The K-means algorithm and the vertical edge map are used to reduce the searching time of the CHT which applied on the edge image to estimate iris center and radius. Therefore, the input image to the CHT is the binary edge image that comes from applying the edge detection on the masked region obtained from K-means. After determining the iris circle, new techniques are applied to isolate the noisy factors like eyelids, eyelashes, luminance and reflections. Finally, the pupil region is removed from the iris region. [Fig. 2](#) shows the steps of the proposed segmentation algorithm. These steps will be explained in details in the following paragraphs.

3.1. Determining iris region

One of the most important sources of error in segmentation is the high local contrast occurring on non-iris regions. These sources may include eyelashes, eyebrow, glass frame or white areas due to luminance on skin behind eye region. Therefore, excluding the non-iris regions before the iris segmentation step avoid such segmentation errors. In other words, if the image is divided into three regions namely iris region, skin region and sclera region, then the errors in segmentation and the searching time are reduced at the overall segmentation process.

Image K-means clustering algorithm is used to divide the eye image into three different regions. The first region which has small intensity values, consists of the iris including the pupil and eyelashes. The second region which has high intensity values, consists of sclera and some highlights or luminance reflections. A third region occurs between the previous two regions is the skin region. The image K-means algorithm is an iterative technique used to divide an image into K clusters by assigning each point to the cluster whose center has the smallest distance. The center is the arithmetic mean of all the points in the cluster. The distance is the absolute difference between a pixel and a cluster center and it is typically based on pixel intensity in our algorithm. The image K-means clustering algorithm is effective because our main concern is the darkest region only. We experimentally found the optimum number of clusters to be three. The basic steps of the image K-means algorithm are

- (1) Compute the intensity distribution.
- (2) Initialize the centroids with k random intensities.
- (3) Repeat the following steps until there is no change in the cluster labels.
- (4) Cluster the points based on distance of their intensities from the centroid.

$$c^{(i)} = \operatorname{argmin}_j \|x^{(i)} - \mu_j\|^2 \quad (1)$$

- (5) Compute the new centroid of each clusters.

$$\mu_i = \frac{\sum_{i=1}^m 1\{c_{(i)}=j\}x^{(i)}}{\sum_{i=1}^m 1\{c_{(i)}=j\}} \quad (2)$$

where i iterates overall the intensities, j iterates overall the centroids and μ_i is the centroids intensities.

In the following paragraphs we will discuss in details the procedures of determining the iris region. First, the red color is separated from the RGB color space of the image, because it contains most of the iris details. Then, the image K-means clustering algorithm is applied on the red color space of the

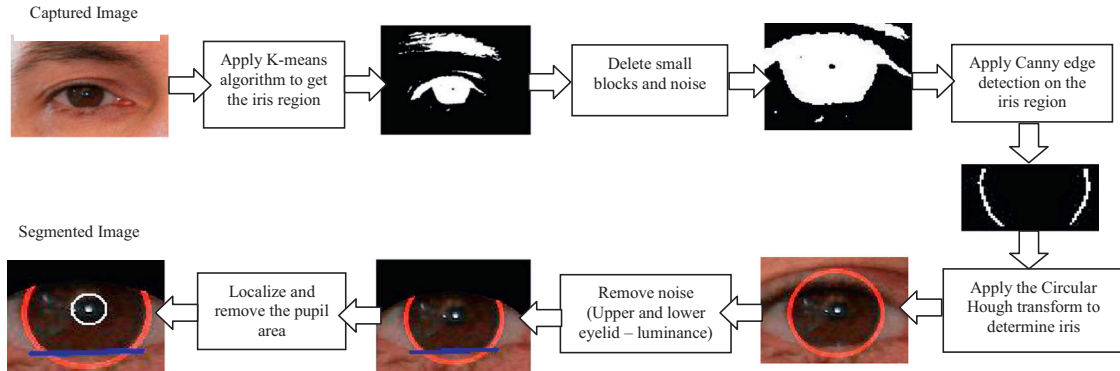


Fig. 2. The stages of the proposed iris segmentation method.

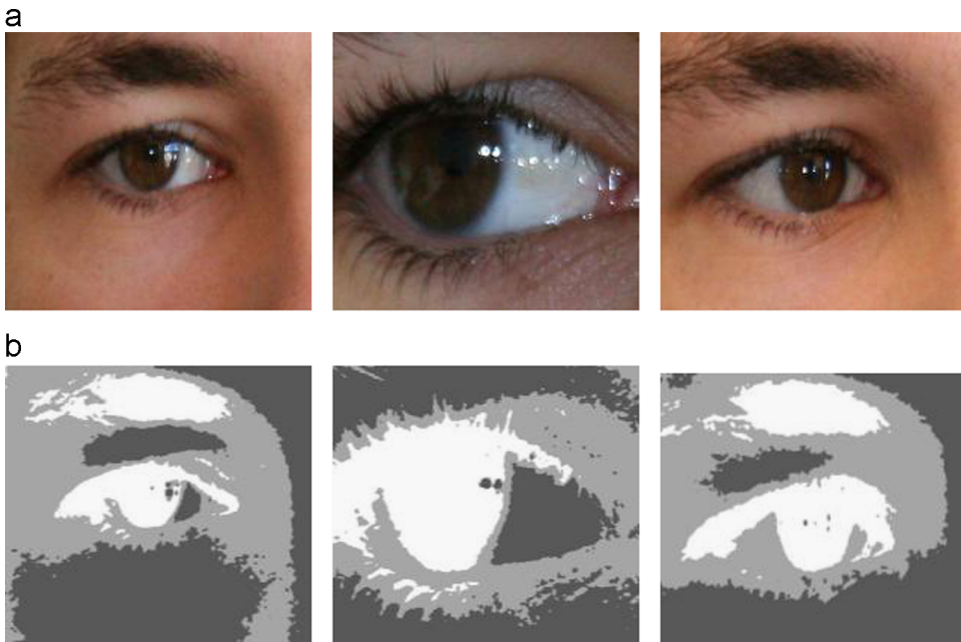


Fig. 3. Illustration the results of K-mean clustering. (a) Real images. (b) Clustering result images, white regions represent the estimated iris region.

image. After clustering, the resulting image is morphologically handled to delete small blocks and noise, of the remaining blocks, the nearest block from the center is used to discard the eyebrow region. Fig. 3 shows the result of applying the clustering algorithm on some images. White regions in Fig. 3(b) present the darkest region, where black regions present the region of sclera and some highlights or luminance reflections, and gray regions are the region of skin. It is seen in Fig. 3 that white area covers the iris, eyelashes and sometimes eyebrow, while excluding luminance and specular reflections. This exclusion is very helpful in reducing the handled pixels by more than 70%. Consequently, the searching time of the next steps will be reduced.

3.2. Detecting edges

To find the edge points in the iris image, Canny edge detection is used [19]. The implemented Canny edge detection has six arguments. The upper threshold and the lower threshold inputs are experimentally adjusted to make the algorithm suitable for the noisy iris images. Because the vertical edges are more significant than the horizontal edges, high value for vertical edges weight and low value for horizontal edges weight are assigned to extract the iris-sclera border. These values are adjusted only once for the

whole database and do not need to be computed for each iris image. This process decreases the errors resulting from the horizontal edges due to eyelashes and eyelids.

Instead of using the grayscale image, it is found experimentally that the Y component of YCbCr color space is the best image that can be used to detect the edges. This is done by converting the RGB iris image to YCbCr color space, and then the Y component is separated. In order to smooth the image and handle small noises, median filter is applied on the Y component image. Note that the edge detection is applied only on the reduced area which resulting from the clustering step. Fig. 4 shows the result of applying the Canny edge detection on sample images. Fig. 4(a) shows the real images and Fig. 4(b) shows the Y component after converting the images to YCbCr color space. It is noted that the Y component reduces the effect of luminance, specular reflection and the red regions in the sclera. As a result, less points are processed in CHT. Fig. 4(c) shows images after applying Canny edge detection. It is seen that the biggest two connected components are the iris boundaries, in spite of the existence of some small noise components which are reduced using morphological operations as shown in Fig. 4(d). It is found that the edge points that will be processed or searched by CHT were reduced by more than 90. Furthermore, the edge points are reduced by scaling the image by factor of 0.5, because it is found that reducing the scale factor to

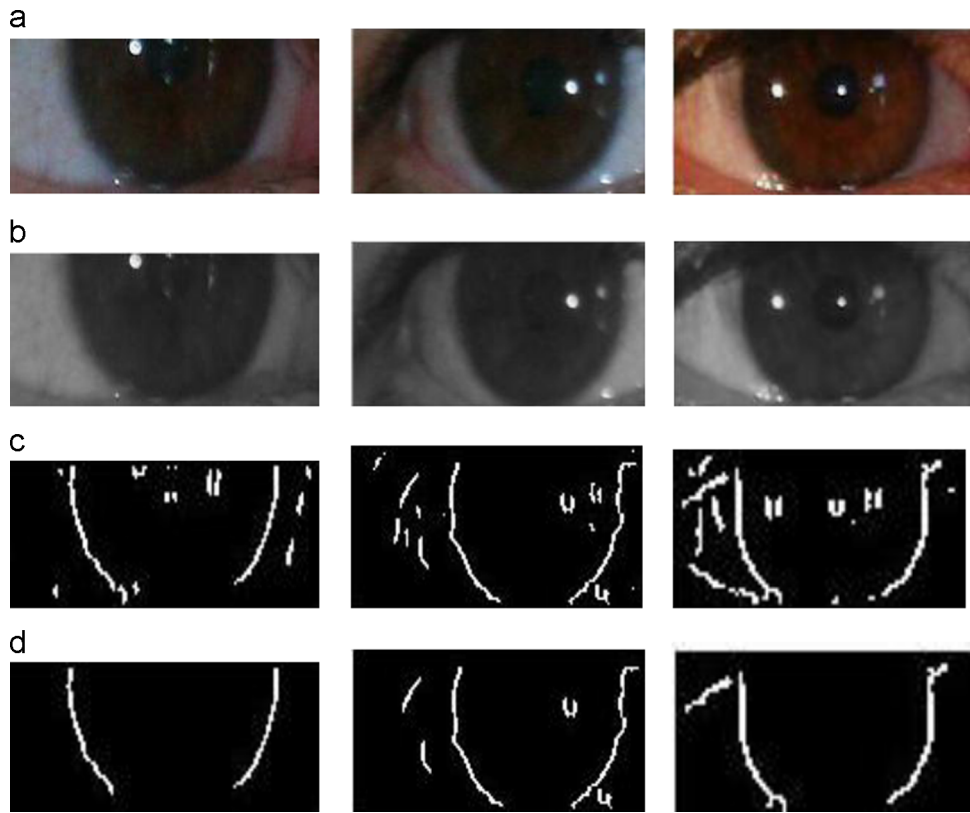


Fig. 4. Illustration the results of applying Canny edge detection on three images (a) Real images. (b) Y component of the image after converting it to YCbCr color space. (c) Binary image resulting from Canny edge detection using scale factor of 0.5 (d) Binary image after removing small blocks and noises.

value less than 0.5, will cause many edge points to disappear and thus cause errors in localizing the iris boundary.

3.3. Applying the circular Hough transform

The CHT [20] belongs to R3 space, so its complexity equals $O(n^3)$. Therefore, three proposed methods which explained in previous steps are used to reduce the execution time:

- (1) Scaling factor: to reduce the image size and cause reduction in the edge points.
- (2) K-means clustering: to reduce the searching area and the edge points when Canny edge detection is applied.
- (3) Morphological operations: to remove small blocks and noise from the binary image.

After applying the CHT on the binary edge image, the maximum group of parameters (a, b, r) is selected from the accumulator, and then the Cartesian parameters (x, y, r) are found to localize the iris. Fig. 5 shows samples of segmented irises from UBIRIS database. As shown in this figure, the iris location boundary is detected and white circles were precisely fit the irises, despite the presence of some noisy factors, like specular reflections, iris occlusion by eyelids and eyelashes. Moreover, it is noted that irises are correctly localized regardless of their size and this is another benefit of the proposed algorithm.

3.4. Isolating noise

In non-cooperative iris recognition, the user has little or even no active participation in the image capturing process [21]. As a result, the iris images are often captured with more noisy factors, such as reflections, occlusions by eyelids or eyelashes, shadows, etc. It has

been reported that the most localization errors occur on non-iris regions due to the high local contrast. Therefore, to avoid such localization errors, the non-iris regions should be excluded and all sources of errors must be handled. In this section, we will explain how the proposed segmentation method handles each of the error sources.

3.4.1. Upper eyelid localization

When iris images are captured in the ideal environments, researchers used many methods to localize the eyelid of the iris e.g. edge detection, Integro-differential operator and Line Hough Transform (LHT). However, these methods are not effective when used in noisy iris images, because the intensity contrast of iris and eyelid can be very low, especially for heavily pigmented dark irises, as that in Fig. 1(a). A new method is proposed to localize the eyelids by detecting them in the sclera region because the intensity contrast between the sclera and the upper eyelid is higher than that between the iris and the upper eyelid. The following steps explain the upper eyelid localization algorithm:

- (1) Isolate two small rectangles from the outer two sides of the iris. Each of these rectangles has a length that equals the iris radius and a width that equals one-third of the iris radius as shown in Fig. 6. The coordinates of the two lower corners of the rectangle on the outer right side of the iris are $(x+r, y), (x+r+r/3, y)$ and the coordinates of the lower corners of the rectangle on the outer left side of the iris are $(x-r, y), (x-r-r/3, y)$ where the point (x, y) is the center of the iris circle and r is the radius of the iris.
- (2) Apply horizontal Canny edge detection on the two rectangles and isolate the noise using morphological operations.
- (3) Determine the coordinates of upper eyelid on both rectangles, assuming that it is the center of the biggest horizontal edge line on each rectangle.

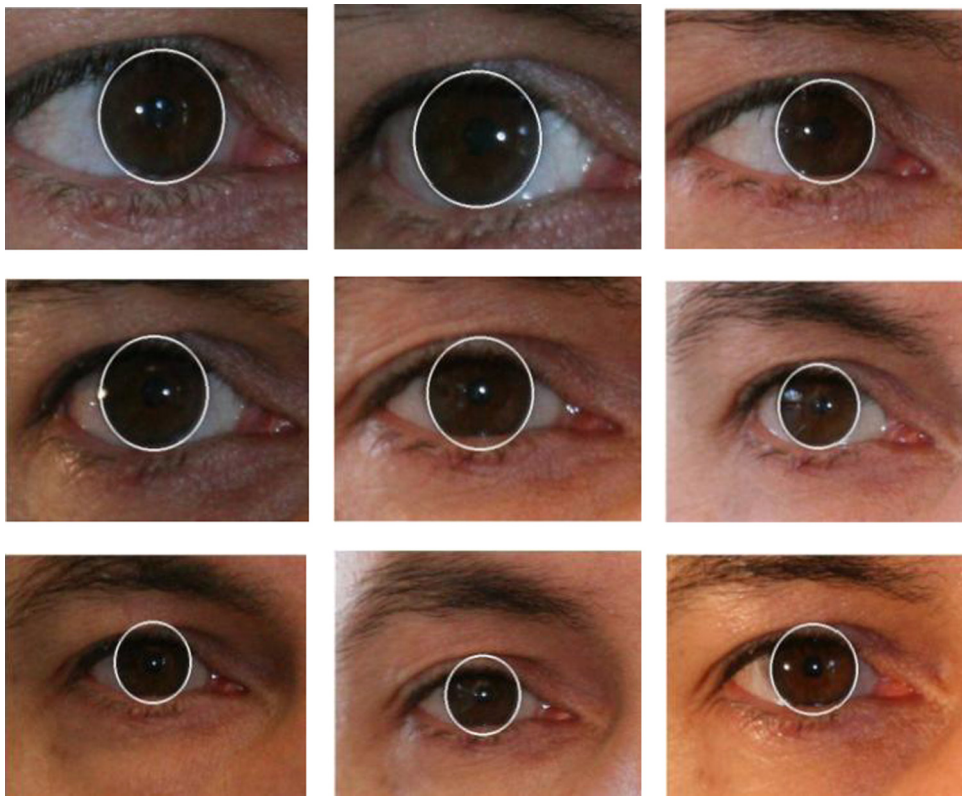


Fig. 5. Samples of segmented irises from UBIRIS database.

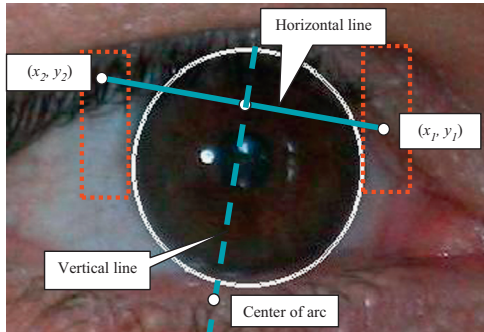


Fig. 6. Upper eyelid localization model.

- (4) Draw an arc that passes through the two coordinates of the upper eyelid on each rectangle with a radius equals double the iris radius. The center of the arc is computed using the following steps:

Let the coordinates of the upper eyelid on the first rectangle be (x_1, y_1) , and coordinates of the upper eyelid on the second rectangle be (x_2, y_2) . The line passing through the two coordinates of the upper eyelid on each rectangle is given by the equation:

$$ax + by + c_{\text{hor}} = 0 \quad (3)$$

where $a = y_2 - y_1$, $b = x_1 - x_2$, $c_{\text{hor}} = x_2y_1 - x_1y_2$. Let (p, q) be the midpoint of the line joining (x_1, y_1) and (x_2, y_2) .

The equation of the perpendicular to the line joining (x_1, y_1) and (x_2, y_2) at the midpoint of these two points is

$$bx - ay + c_{\text{vert}} = 0 \quad (4)$$

where $c_{\text{vert}} = aq - bp$. Then, the distance between the arc center and the middle of the line joining (x_1, y_1) and (x_2, y_2) is twice the iris radius as shown in Fig. 6.

Fig. 7 shows sample images of UBIRIS v2 and v1 after using the proposed method to localize the upper eyelid of the iris. Note that, due to the use of the arc in the proposed algorithm, the iris region will not lose non-noise regions as in using the LHT algorithm. It is seen in **Fig. 7** that the proposed algorithm isolated the upper eyelid accurately, even if the very low intensity contrast between the iris and the eyelid, whereas the normal algorithms like LHT and Integro-Differential operator of Daugman cannot isolate it.

The effectiveness of the proposed algorithm is due to the usage of the intensity contrast between the sclera and the upper eyelid rather than the iris and the upper eyelid, therefore the algorithm overcomes the segmentation errors resulting from low intensity contrast between the iris and the upper eyelid. Furthermore, in contrast to other algorithms the proposed algorithm is still working, when a huge area of iris is occluded by upper eyelid.

3.4.2. Lower eyelid localization

To localize the lower eyelid of the iris, the LHT is used because most of the lower eyelid occlusions are approximately linear. First, the Canny edge detection is applied to the lowest half of the iris and then the best line is found using LHT. If the vote of the line is less than a certain value, then we assume that lower eyelid occlusions do not occur.

Fig. 8 shows some examples after localizing the lower eyelid. The blue line represents the largest edge line that separates the iris and the lower eyelid. It is known that the lower eyelid isolation process is easier than that of the upper eyelid because there is no eyelashes occlusion and the occluded area of the iris due to the lower eyelid is usually less than that due to the upper eyelid.

3.4.3. Specular reflections isolations

Specular reflections can be a serious problem when there are noisy images processed by the iris recognition system. A new simple reflection removal method is proposed in two steps:

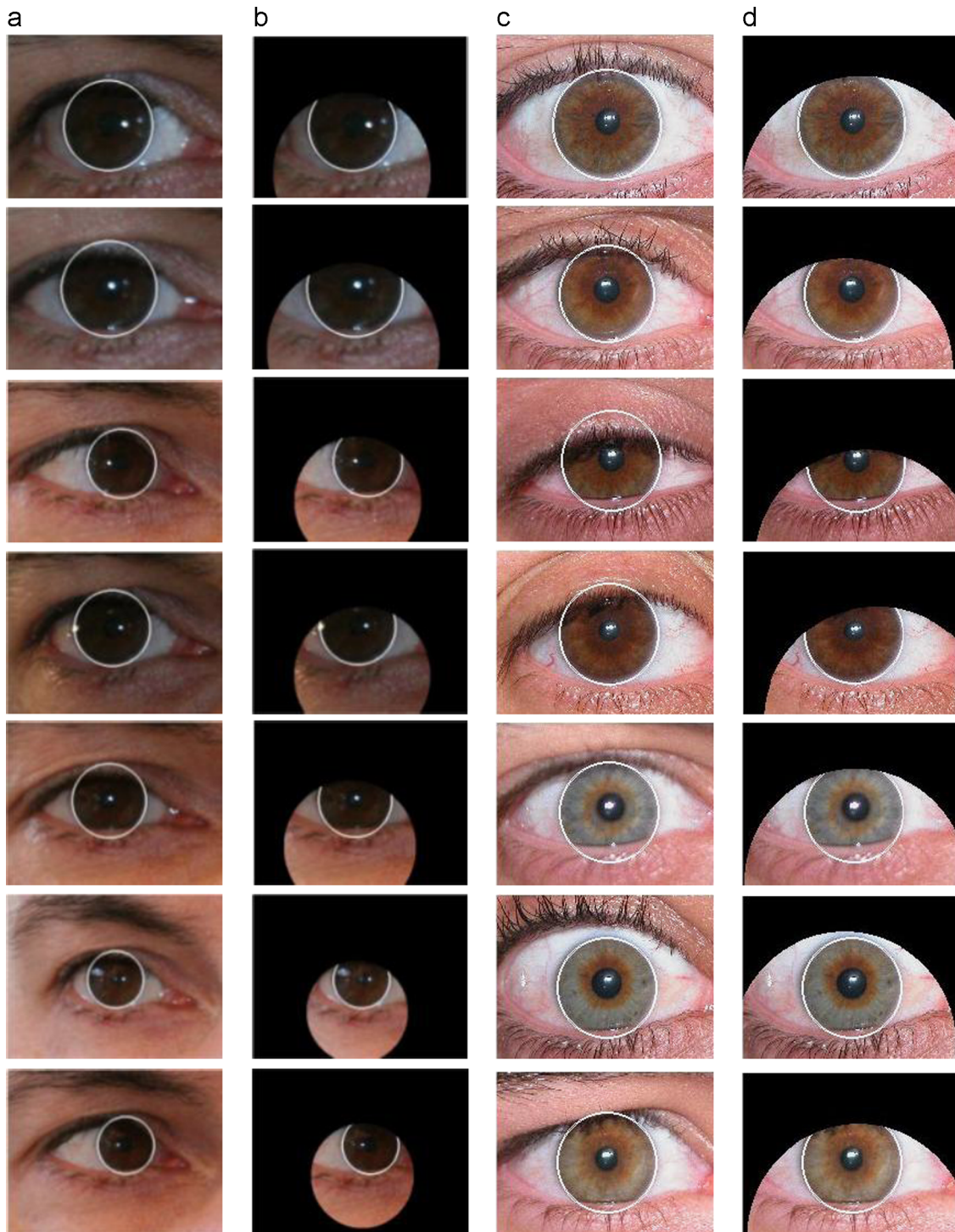


Fig. 7. Upper eyelid localization algorithm (a) segmented images from UBIRIS v2. (b) segmented images from UBIRIS v2 after using the proposed upper eyelid localization. (c) segmented images from UBIRIS v1. (d) segmented images from UBIRIS v1 after using the proposed upper eyelid localization.

- (1) Compute the average intensity of the iris region in the three RGB color spaces (After upper and lower eyelids removal).
- (2) Test the intensity of each pixel in the iris, and if the intensity of the pixel in certain color space is greater than the average intensity computed in the first step plus constant value, then consider this pixel as a reflection noise. The constant value is adjusted only once for the whole iris database.

Fig. 9 shows some images after localizing the specular reflections. The pixels which are marked with a red color are masked to be isolated, when iris template code is extracted. The specular

reflection and highlight regions are determined precisely even in the presence of light reflection or small occluded regions as shown in Fig. 9. Note that this process can also discard some redundant white spaces that might result from off-angle captured images.

3.4.4. Pupil region removing

Pupil removal is performed in the last step because one of the major differences between the eye images in the noisy databases were captured under visible wavelengths and with those taken under Near Infrared illumination is that the intensity contrast of

the iris and the pupil is very low, especially for heavily pigmented irises as shown in Fig. 6. If we try to localize the pupil in noisy images directly, the segmentation will fail because the darkness of the iris. Therefore the best method is to enhance the image iris to make the pupil more visible using the contrast enhancement method [22]. The following steps explain the pupil removal process:

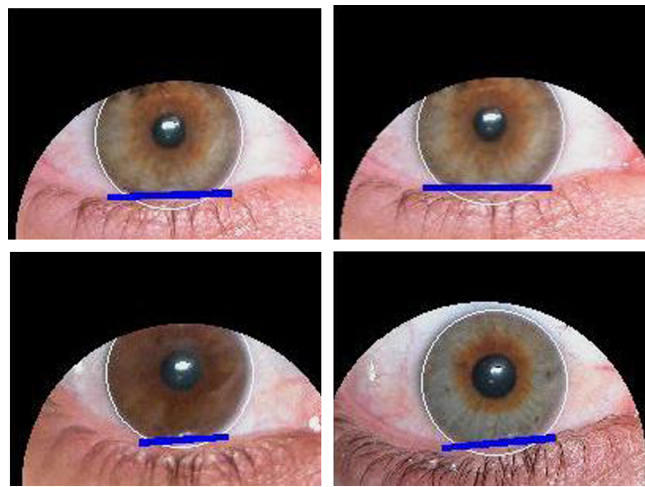


Fig. 8. Lower eyelid localization samples using UBIRIS v1 database.

- (1) Adjust iris image by mapping the intensity values of its bits to new values to focus on dark intensities. This step makes the difference between the iris and the pupil more clear.
- (2) Apply median filter to reduce the noisy factors and to preserve the edges.
- (3) Use Canny edge detection to get the edge map.
- (4) Apply the CHT to localize the pupil, assuming that it is circular. The pupil radius is set to be in the range of 1/10–7/10 of the iris radius.

Fig. 10 shows the steps of this algorithm using an image from UBIRIS v2. Note that all previous steps are applied only on a square inside the iris to reduce the execution time and to avoid errors that may happen due to the edge points that lays outside the pupil region. The center of this square is the same of the iris and the coordinates of the left corner of the square is $(x-r/2, y-r/2)$ where the point (x, y) is the iris center and r is the iris radius. As shown in Fig. 10, the pupil localization succeeds even with very low intensity contrast between the iris and the pupil.

Fig. 11 shows the behavior of the proposed segmentation algorithm on image sequences taken in real-conditions from UBIRIS iris image database. As illustrated in previous sections, the K-means algorithm determines the iris region which is marked with the blue rectangle in Fig. 11(c) and the Canny edge detection is applied on this region only. The result is a small number of edge points as in Fig. 11(d) which makes the CHT work faster. In Fig. 11(f), the eyelids, the pupil and the luminance are removed using proposed algorithms. It

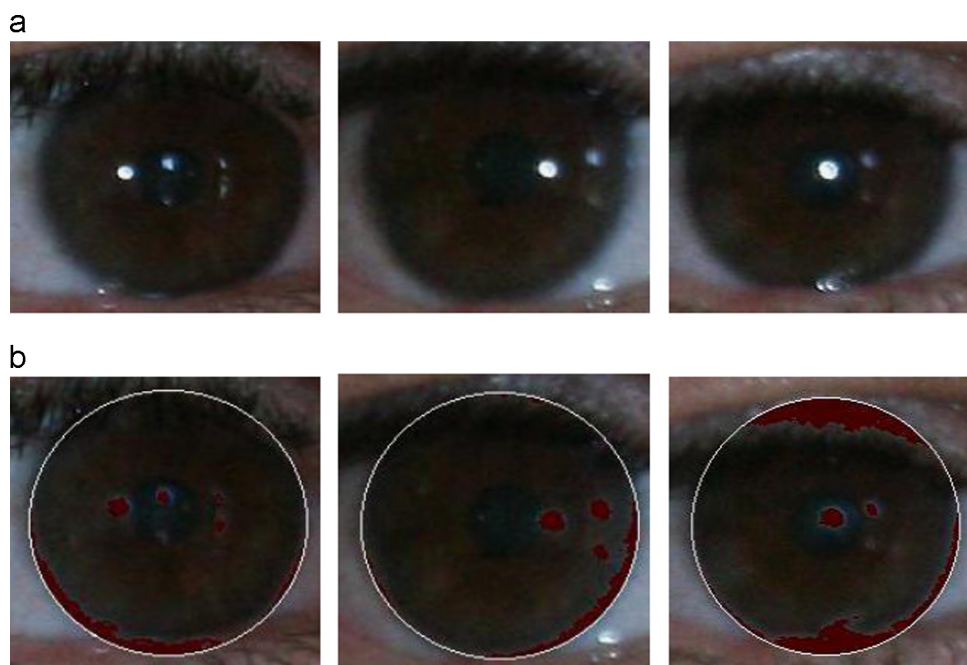


Fig. 9. Isolating reflections from irises in the proposed algorithm (a) image with reflections. (b) detect the reflection regions (marked with red color).

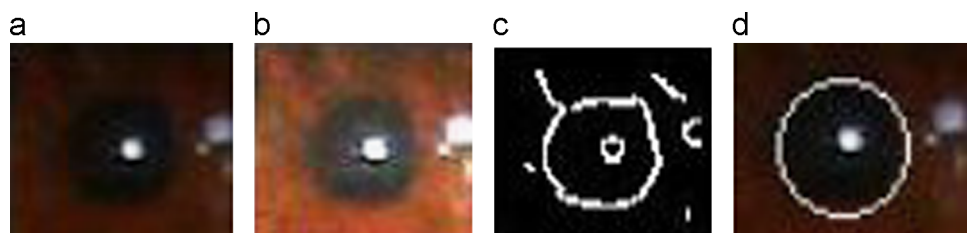


Fig. 10. Steps of Pupil removal algorithm (a) the inner square of the iris. (b) result of adjust image in (a). (c) result of Canny edge detection. (d) result of CHT.

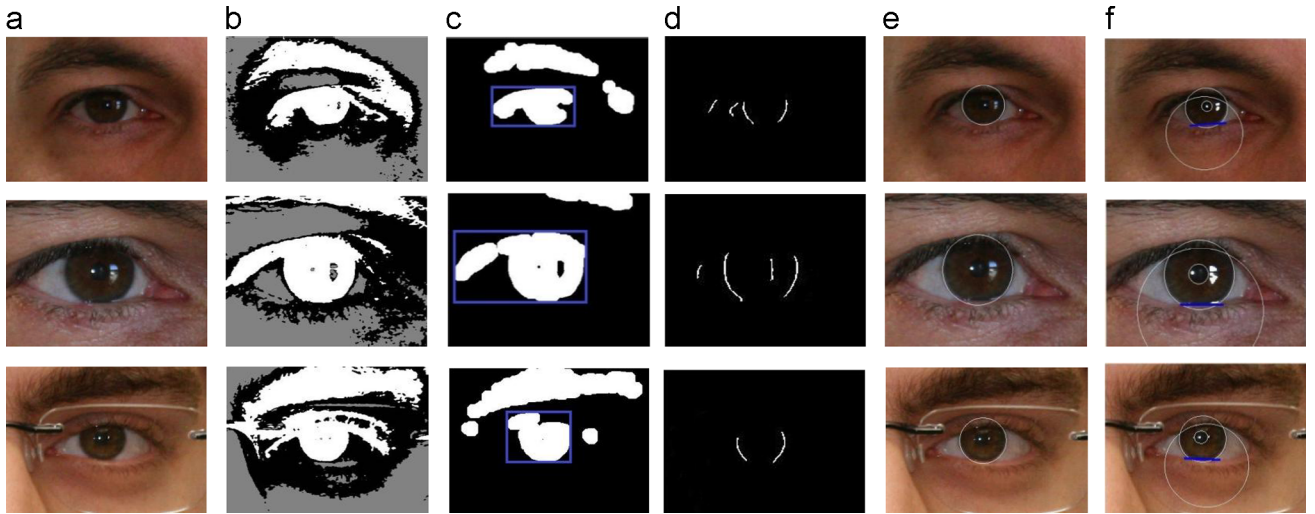


Fig. 11. The behavior of the proposed segmentation algorithm on image sequences taken in real-conditions from UBIRIS iris image database.(a) the real image. (b) the binary image after applying the K-means. (c) the clustered binary image after applying some morphological operations. (d) the edge map image after applying the Canny algorithm on the estimated iris region. (e) the image after localizing the iris using CHT. (f) the image after removing the noise regions.

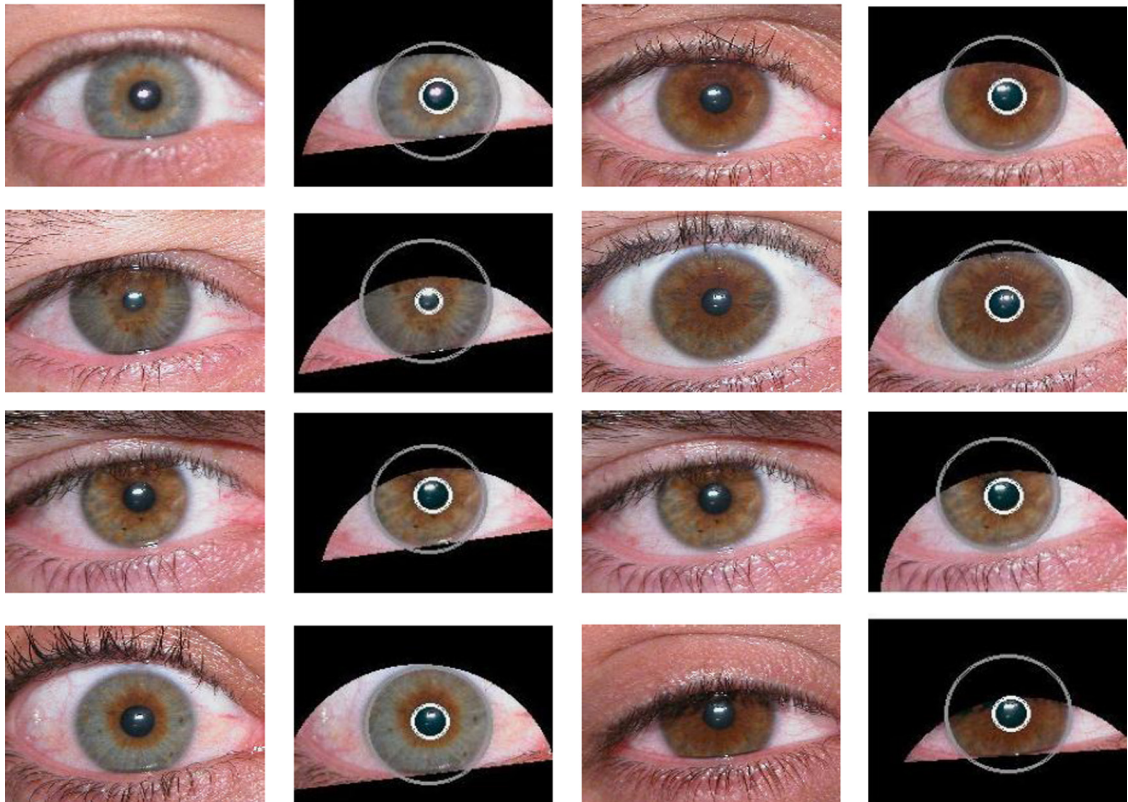


Fig. 12. Examples of correct segmented irises.

is clear that the proposed algorithm succeed in segmenting iris images even in the presence of noise types such as iris obstructions, specular reflection and glasses.

4. Experimental results

To evaluate the proposed segmentation algorithm, it is implemented using MATLAB 7.0 software. The environment where the experiments were conducted is Compaq PC, Core 2 Due Intel Pentium Processor (2.00 GHz), with 1GB RAM and Windows 7 operating

system. We start the implementation with K-means clustering followed by edge detection and CHT as shown in Fig. 2. It is assumed that both the iris and the pupil have circular forms, therefore every circle is completely described by the values of its center (x, y) and radius r .

UBIRIS v1 (Session 1) [26] iris database is used to evaluate the proposed segmentation algorithm. This database is composed of 1877 images collected from 241 eyes. It simulates unconstrained imaging conditions. Fig. 12 shows the segmented images after applying the proposed iris segmentation algorithm on UBIRIS v1 database. The accuracy and the average segmentation time are

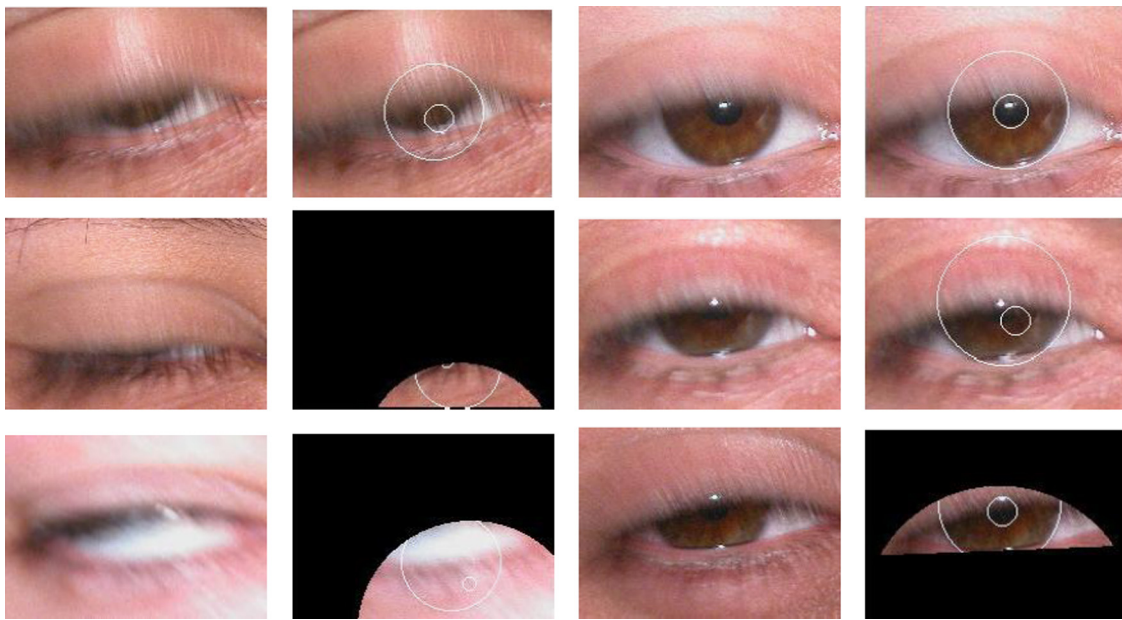


Fig. 13. Examples of failed segmented noisy irises when eyelids and eyelashes obstruct a big portions of the iris.

Table 1

Comparison between the accuracy of proposed algorithm and some previous algorithms.

Method	Accuracy	Time (s)
Daugman	95.22%	2.73
Wildes	98.68%	1.95
Camus and Wildes	96.78	3.12
Martin-Roche	77.18%	–
Fourier spectral [28]	98.49 (limbic) 94.47 (pupil)	–
Proposed	98.76%	1.49

computed for the proposed algorithm and some previous algorithms [23]. The segmentation is considered accurate when the following two conditions are provided:

- (1) The two circles of the iris and the pupil fall exactly into the iris and the pupil borders of the resulting images.
- (2) The upper and the lower eyelids are correctly localized.

If any of the two previous conditions is not satisfied, then the segmentation is not accurate as shown in Fig. 13. The average segmentation time is computed by calculating the segmentation time for all the correctly segmented iris images in the dataset divided by the number of the correctly segmented iris images. Table 1 shows comparison between the accuracy of proposed algorithm and some previous algorithms.

As shown in the table, the accuracy of the proposed algorithm is better than Daugman and Wildes algorithms. Meanwhile, the execution time of our segmentation algorithm is the lowest one because of applying the proposed steps to reduce the searching areas in CHT. Wildes used multi-resolution coarse-to-fine search approach, and searches over the hole iris image pixels without any preprocessing techniques which take more time than the proposed algorithm. The Fourier spectral algorithm got good results in limbic localization but the error is high in pupil localization, which increase the total segmentation error. The proposed algorithm failed in segmenting noisy irises when eyelids and eyelashes obstruct big portions of the iris (more than 60%) or when the upper or lower eyelids cover the pupil of the iris (Note that most segmentation methods fail in these cases). Fig. 13 gives examples

of iris images which the proposed algorithm failed to segment. In the second column of Fig. 13, the proposed segmentation algorithm failed because the iris is almost covered by eyelids. In the fourth column, the proposed segmentation algorithm succeeded in localizing the iris boundary, but it failed in localizing the pupil boundary when it is covered by eyelids. Further, it failed in isolating the eyelids regions when the iris image is blurred due to fast movements while capturing the image.

To evaluate the performance of the proposed segmentation method in the whole recognition system, the other three stages (normalization, encoding, comparisons) is implemented. Some functions from Masek iris recognition algorithm are used [24]. The implemented system is used to generate the iris template code for every iris. To plot the match and non-match distributions for this database, each iris image is compared with the other all irises in the database. For the UBIRIS v1 (session1) iris database, the total number of comparisons equals 1,448,410 where the total number of intra-class comparisons equals 2410 and that of inter-class comparisons equals 1,446,000.

During the comparison stage, the Hamming Distance (HD) is used as the metric of dissimilarity between two considered iris codes $codeA$ and $codeB$:

$$HD = \frac{\|(codeA \otimes codeB) \cap maskA \cap maskB\|}{\|maskA \cap maskB\|} \quad (5)$$

where $maskA$ and $maskB$ are the masks of $codeA$ and $codeB$, respectively. A mask as proposed by Daugman [17] signifies whether any iris region is occluded by eyelids, eyelashes, luminance, etc. HD is therefore a fractional measure of dissimilarity after noise regions are removed.

Fig. 14 shows the distribution of the HD when the proposed segmentation algorithm is used and Fig. 15 shows the distribution of the HD when Daugman segmentation algorithm is used. The results show that the match distribution when the proposed algorithm was used has shifted a significant distance to the left and the mean of the match distribution has decreased by 0.12. In Fig. 15 when Daugman algorithm is applied, the distance between the two means equals 0.075 and the distance between the two means in Fig. 14 when proposed algorithm is applied equals 0.19. It is seen that the distance between the match and non-match distribution increase when the proposed segmentation algorithm

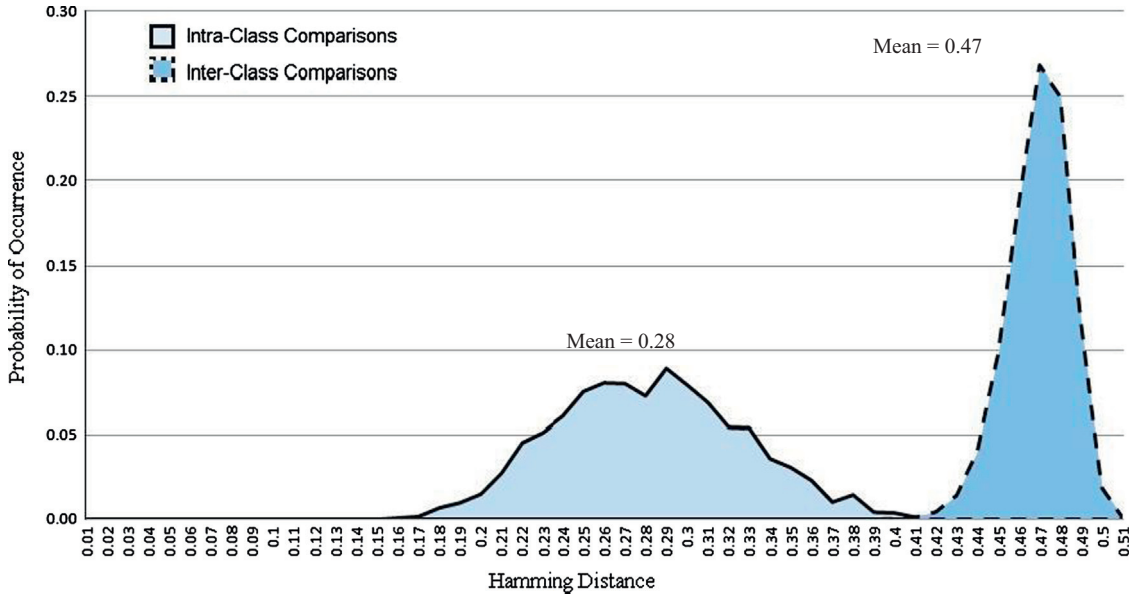


Fig. 14. The match and non-match distributions for UBIRIS v1 when the proposed segmentation algorithm is used.

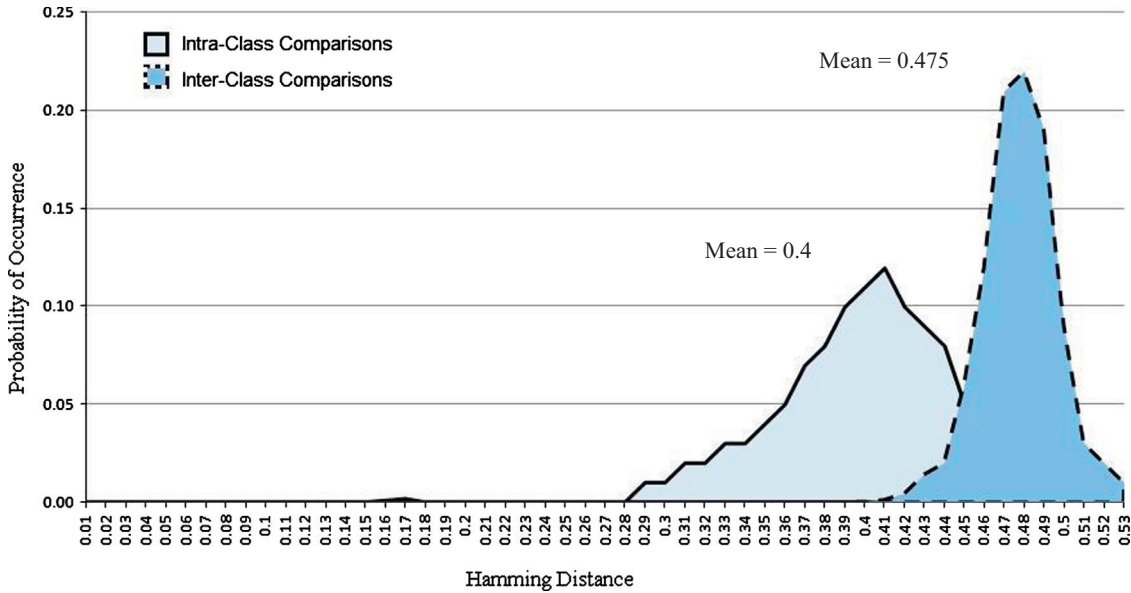


Fig. 15. The match and non-match distributions for UBIRIS v1 when Daugman algorithm is used.

is used. As a result, the error rates will decrease and a large improvement over Daugman algorithm performance is achieved. Moreover, it is noticed that when the proposed segmentation algorithm is used, the interference of the match and non-match distribution is less than that when Daugman segmentation algorithm is used. This is because the Daugman segmentation algorithm is very sensitive to noise and cannot handle noisy factors which occur in non-ideal conditions such as specular reflections, pupil isolation and eyelids occlusion.

Fig. 16 shows the EER of iris recognition system when our proposed algorithm is used. EER is the point at which FMR and FNMR are almost equal. FMR occurs when the system accepts an identity claim, but the claim is not true. FNMR occurs when the system rejects an identity claim, but the claim is true. EER enables evaluation of FMR and FNMR at a single operating point and the lower the EER value is, the higher the accuracy of the biometric system will be. When the proposed segmentation algorithm is used, the EER is 0.126 which is a low value

comparing with EER value of the latest iris recognition systems which range from 3.6% to 0.07% as described in [27]. This result shows that the proposed segmentation algorithm accurately isolates error regions in iris template. Thus, the FMR and FNMR will decrease. The other segmentation algorithms like Daugman cannot handle these sources of error because it is designed to work under ideal conditions and use the Integro-Differential operator which frequently fails when the images do not have sufficient intensity separability between the iris and the sclera.

To evaluate the performance of the proposed segmentation algorithm over different techniques, Daugman's method is implemented using some functions from Masek's iris recognition algorithm [24] and the results of applying SVM Match Score Fusion algorithm [25] are used. We use the most important points which are FAR(%) at 0.0001% FRR and FRR(%) at 0.0001% FAR to compare our algorithm with others. Where the FRR is the probability that the system fails to detect a match between the input pattern and a

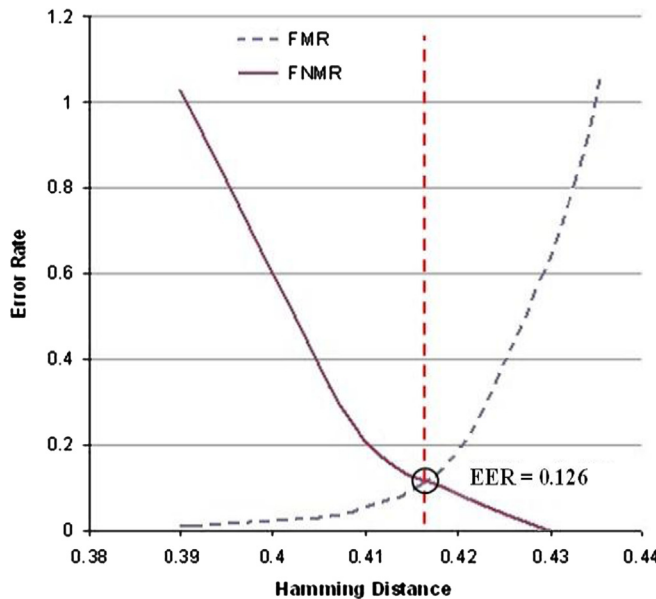


Fig. 16. The Equal Error Rate value where FMR and FNMR are equal.

Table 2
Comparison of the proposed algorithm with two previous algorithms.

Method	FAR(%) at 0.0001% FRR	FRR(%) at 0.0001% FAR
Daugman	7.2	12.96
SVM Match Score Fusion	5.9	8.71
Proposed	1.5	5.82

matching template in the database, and the FAR is the probability that the system incorrectly matches the input pattern to a non-matching template in the database.

The results of the three algorithms are summarized in **Table 2**. It is shown that the proposed segmentation algorithm significantly reduces the two metric values. At 0.0001% FRR, the proposed algorithm reduces the FAR by 5.7% when Daugman algorithm is used and by 4.4% when SVM algorithm is used. Whereas at FAR of 0.0001%, the proposed algorithm reduces the FRR by 7.14% when Daugman algorithm is used and by 2.89% when SVM algorithm is used. This means that the proposed algorithm could reduce the error in the two common security cases, the first case when the cost of FRR error may exceed the cost of FAR error such as in a customer context, the second case when the cost of FAR error may exceed the cost of FRR error such as in the military context. These improvements in the performance of the iris recognition system when the proposed segmentation algorithm is used are due to its ability to handle many types of errors which might occur in non-ideal environments.

5. Conclusion

This research proposed a new effective and fast algorithm to segment the non-ideal iris images captured under unconstrained imaging conditions which generate several types of noises, such as iris obstructions and blurred iris images. The proposed algorithm added a new pre-processing step to segmentation steps which is clustering the iris image using K-means algorithm. This pre-processing step excludes from the image the non-iris regions which cause many errors and decrease the searching time in the

next steps. CHT is applied to the binary edge map on the estimated iris region to localize the outer iris borders. A new method to localize the upper eyelids is proposed by detecting it in the sclera region. To localize the lower eyelid of the iris LHT is used because most occlusions of the lower eyelid is approximately linear. Finally, in order to remove the pupil region, iris image is adjusted by mapping its bits intensity values to new values to focus on dark intensities and then CHT is applied. Experimental results on UBIRIS iris database indicate the high accuracy and less execution time of the proposed segmentation algorithm compared with previous algorithms.

Conflict of interest statement

None declared.

References

- [1] J. Daugman, Statistical richness of visual phase information: update on recognizing persons by their iris patterns, *International Journal of Computer Vision* 45 (1) (2001) 25–38.
- [2] J. Daugman, Demodulation by complex-valued wavelets for stochastic pattern recognition, *International Journal of Wavelets, Multiresolution and Information Processing* 1 (1) (2003) 1–17.
- [3] R. Wildes, Iris recognition: an emerging biometric technology, *Proceedings of the IEEE* 85 (1997) 1348–1363.
- [4] L. Flom, A. Safrir, Iris Recognition System, US Patent 4641394, 1987.
- [5] J. Daugman, Biometric Personal Identification System Based on Iris Analysis, United States Patent, Patent Number: 5,291,560, 1994.
- [6] J.G. Daugman, High Confidence Visual Recognition of Persons by a Test of Statistical Independence, *IEEE Transactions on Pattern Analysis and Machine Intelligence* 15 (11) (1993) 1148–1161.
- [7] A. Ross, S. Shah, Segmenting non-ideal irises using geodesic active contours, in: *Proceedings of the IEEE 2006 Biometric Symposium*, 2006, pp. 1–6.
- [8] R. Donida Labati, V. Piuri, F. Scotti, Agent-based image iris segmentation and multipleviews boundary refining, in: *Proceedings of the IEEE Third International Conference on Biometrics: Theory, Applications and Systems*, November 20, 2009.
- [9] Y. Chen, M. Adjouadi, CA Han, J. Wang, A. Barreto, N. Rishe, J. Andrian, A highly accurate and computationally efficient approach for unconstrained iris segmentation, *Image and Vision Computing* (2010).
- [10] M. Vatsa, R. Singh, A. Noore, Improving iris recognition performance using segmentation quality enhancement match score fusion and indexing, *IEEE Transactions on Systems, Man, and Cybernetics* 38 (4) (2008) 1021–1035.
- [11] H. Proenca, L.A. Alexandre, Iris segmentation methodology for non-cooperative recognition, *IEE Proceedings of Vision, Image and Signal Processing* 153 (2) (2006) 199–205.
- [12] X. Liu, K.W. Bowyer, P.J. Flynn, Experiments with an Improved Iris Segmentation Algorithm, in: *Proceedings of the 4th IEEE Workshop on Automatic Identification Advanced Technologies*, 2005, pp. 118–123.
- [13] M. Dobes, J. Martineka, D.S.Z. Dobes, J. Pospisil, Human eye localization using the modified Hough transform, *Optik—International Journal for Light and Electron Optics* 117 (2006) 468–473.
- [14] S. Schuckers, N. Schmid, A. Abhyankar, V. Dorairaj, C. Boyce, L. Hornak, On techniques for angle compensation in nonideal iris recognition, *IEEE Transactions on System, Man, and Cybernetics—Part B: Cybernetics* 37 (5) (2007) 1176–1190.
- [15] T. Tan, Z. He, Z. Sun, Efficient and robust segmentation of noisy iris images for non-cooperative iris recognition, *Image and Vision Computing* 28 (2010) 223–230.
- [16] J. Zuo, N. Kalka, N. Schmid, A robust iris segmentation procedure for unconstrained subject presentation, in: *Proceedings of the Biometric Consortium Conference*, 2006, pp. 1–6.
- [17] J. Daugman, New methods in iris recognition, *IEEE Transactions on System, Man, and Cybernetics—Part B: Cybernetics* 37 (5) (2007) 1167–1175.
- [18] T.A. Camus, R. Wildes, Reliable and fast eye finding in close-up images, in: *Proceedings of the IEEE 16th International Conference on Pattern Recognition*, Quebec, August 2002, pp. 389–394.
- [19] J. Canny, A computational approach to edge detection, *IEEE Transactions on Pattern Analysis and Machine Intelligence* 8 (1986) 679–698, Nov..
- [20] D. Ballard, Generalized Hough transform to detect arbitrary patterns, *IEEE Transactions on Pattern Analysis and Machine Intelligence* (1981) 111–122.
- [21] H. Proenca, L.A. Alexandre, The NICE I: Noisy Iris Challenge Evaluation—Part I, in: *Proceedings of the First International Conference on Biometrics: Theory, Applications, and Systems*, 2007, pp. 1–4.
- [22] K. Delac, M. Grgic, A survey of biometric recognition methods, in: *Proceedings of the 46th International Symposium Electronics in Marine, ELMAR-2004*, Croatia, June 2004, pp. 184–193.

- [23] Hugo Proenca, Towards non-cooperative biometric iris recognition (PhD thesis), University of Beira Interior, October 2006.
- [24] L. Masek, P. Kovesi, MATLAB source code for a biometric identification system based on iris patterns, The University of Western Australia, 2003. (<http://www.csse.uwa.edu.au/~pk/studentprojects/libor/>).
- [25] M. Vatsa, R. Singh, A. Noore, Improving iris recognition performance using segmentation, quality enhancement, match score fusion, and indexing, Presented at IEEE Transactions on System, Man, and Cybernetics–Part B, 2008, pp. 1021–1035.
- [26] H. Proençá, L. A. Alexandre, UBIRIS: a noisy iris image database, in: Proceedings of the 13th International Conference on Image Analysis and Processing, ICIAP2005, Calgary, September 2005, pp. 970–977.
- [27] Kevin W. Bowyer, Karen Hollingsworth, Patrick J. Flynn, Image understanding for iris biometrics: a survey, Computer Vision and Image Understanding 110 (2) (2008) 281–307.
- [28] Niladri B. Puhan, N. Sudha, Anirudh S. Kaushalram, Efficient segmentation technique for noisy frontal view iris images using Fourier spectral density, 2011.

Shaaban Sahmoud received the BS degrees in Computer Engineering in 2006, from the Islamic University of Gaza, Palestine. He obtained a Master of Philosophy from the same university in 2011 in the field of pattern recognition. His research interests include computer vision, image processing, pattern recognition and artificial intelligence. He is a teaching assistant at the University Collage of Applied Sciences, Gaza, Palestine.

Prof. Abuhaiba is a professor at the Islamic University of Gaza, Computer Engineering Department. He obtained his Master of Philosophy and Doctorate of Philosophy from Britain in the field of document understanding and pattern recognition. His research interests include computer vision, image processing, document analysis and understanding, pattern recognition, artificial intelligence. Furthermore, Prof. Abuhaiba is open-minded and can do and supervise research in all fields of computer engineering, computer science, information systems, and related fields. Prof. Abuhaiba presented important theorems and more than 30 algorithms in document understanding. He published several original contributions in the field of document understanding in well-reputed international journals and conferences. Because of the reference value of Prof. Abuhaiba's achievements, Marquis Who's Who has selected his biographical profile for inclusion in the 23rd (2006) Edition of Who's Who in the World. This edition features biographies of 50,000 of the most accomplished men and women from around the globe and across all fields of endeavor.